

## Effects of signs in tunneling matrix elements on transmission zeros and phase

Tae-Suk Kim<sup>1</sup> and S. Hershfeld<sup>2</sup><sup>1</sup> School of Physics, Seoul National University, Seoul 151-747, Korea<sup>2</sup> Department of Physics, University of Florida, Gainesville FL 32611-8440

(Dated: March 22, 2024)

The effect of the signs in the tunneling matrix elements on the transmission zeros and the transmission phase in transport through a quantum dot is studied. The existence of transmission zeros is determined by both the relative signs and the strength of the tunneling matrix elements for two neighboring energy levels of a dot. The experimentally observed oscillating behavior of the transmission phase over several Coulomb peaks can be explained by a uniform distribution of the relative signs. Based on a simple model of a quantum dot, we present a possible scenario which can give such uniform signs over several conductance peaks. We suggest that the location of the transmission zeros can be identified by inspecting the Fano interference pattern in the linear response conductance of a closed Aharonov-Bohm (AB) interferometer with an embedded quantum dot as a function of the number of electrons in the dot and the AB flux.

PACS numbers: 73.63.Kv, 85.35.Ds, 03.65.Vf

## I. INTRODUCTION

Landauer's scattering theory has been very successful in understanding transport phenomena in the mesoscopic systems. Electrons, when scattered, experience a phase shift in their wave functions and this phase shift (Friedel phase) is stored in the scattering matrix. Though the transmission amplitude contains information about both its magnitude and phase (transmission phase), the conductance measures only the absolute value of the transmission amplitude. Recently a number of experiments have measured the phase shift experienced by electrons passing through a quantum dot, using Aharonov-Bohm (AB) interferometers<sup>1,2,3,4</sup>. The measured phase is not the Friedel phase as we know in bulk systems, but the transmission phase which is the argument of the transmission amplitude through a quantum dot. In a closed AB interferometer, the measured phase is constrained to be either 0 or  $\pi$  as a consequence of the Onsager relations. The phase is observed to jump by  $\pi$  at the conductance peaks and remains in phase between successive Coulomb peaks<sup>1</sup>.

In order to observe the phase evolution in a quantum dot, an open AB interferometer similar to the double-slit experiments was devised by Schuster, et. al.<sup>2</sup>. The measured phase evolves smoothly by  $\pi$  over the Coulomb peaks, which can be expected for resonant tunneling. The transmission phase jumps by  $\pi$  somewhere in between two neighboring peaks and remains in phase between successive Coulomb peaks. This unexpected sudden phase jump can be understood in terms of the transmission zeros.<sup>5,6,7</sup> Oscillating behavior of the phase  $\phi$  as a smooth increase over the Coulomb peaks and a sudden drop in between  $\phi$  is observed over several successive Coulomb peaks.

In this paper we study theoretically the effects of the signs of the tunneling matrix elements between a quantum dot and two leads on the transmission probability  $T_0$  of a quantum dot. Silva, Oreg, and Gefen have recently

shown that the signs of the tunneling matrix elements play a crucial role in determining the behavior of the transmission probability and phase by studying a quantum dot with two resonant levels.<sup>8</sup> A number of other works have either explicitly or implicitly addressed the role of the relative sign of the tunneling matrix elements.<sup>9</sup> In this paper, we consider quantum dots with many levels and consider several possible distributions of the signs in the tunneling matrix elements for each energy level in a quantum dot. The effects of a given distribution of the signs on the transmission phase and zeros is studied. Although the distribution of the signs in the tunneling matrix elements is computed for one simple model, the emphasis here is on understanding the general relationship between the transmission phase and the relative signs of the matrix elements. This can be used, for example, to work backward from experiment to determine the relative signs of the tunneling matrix elements. Not all distributions of the relative signs of the tunneling matrix elements may be physically realizable. It is still an open question why the phase jump or the transmission zeros show up over the energy range of several Coulomb peaks. Transmission zeros can arise from the interference between the possible current paths through the multiple energy levels in a dot, and can explain the abrupt phase jump by  $\pi$ .

We find from our model study that the oscillating behavior in the transmission phase is a result of having the same relative signs in the tunneling matrix elements. Successive transmission zeros in some energy interval arise when the relative signs in the left and right tunneling matrix elements are the same for all the energy levels lying inside that interval. The well-studied stub<sup>6,7,10</sup> belongs to this category. The transmission zeros are absent from the interested energy interval when the relative signs oscillate from level to level. In this case, the transmission phase steadily increases by  $\pi$  over every peak in  $T_0$ . The double-barrier well<sup>6,7,10</sup> shows this type of structure in the transmission amplitude. These

results are in agreement with those found earlier in two level quantum dots.<sup>8</sup>

Based on studying several different cases for the relative signs of the tunneling matrix elements, we are able to deduce simple rules governing the presence or absence of transmission zeros when the tunneling matrix elements are much smaller than the interlevel energy spacing. In addition depending on the distribution of signs, the transmission probability in an AB interferometer with an embedded dot takes on unique shape, especially as a function of the Aharonov-Bohm flux. Thus, complementary to the direct measurements of the transmission phase in the open AB interferometer, we suggest that the position of transmission zeros of the quantum dot can be located by inspecting the Fano interference pattern in the linear response conductance.

The rest of this paper is organized as follows. In Sec. II, the model Hamiltonians and the formalism are described. We present our results of four model studies in Sec. III and discuss a particular model for the relative signs of the matrix elements in Sec. IV. Our study is summarized and concluded in Sec. V. In the Appendix, the case of a complex Fano asymmetry factor in an AB ring geometry is discussed.

## II. MODEL AND FORMALISM

To study the effect of the signs of the tunneling matrix elements between a quantum dot and two leads on the transmission probability and phase, we consider a quantum dot which is modeled by discrete single-particle energy levels and is connected to two metallic leads by tunneling. The metallic leads can accommodate only one transport channel. The model Hamiltonian is given by the equation,  $H = H_0 + H_1$ , where

$$H_0 = \sum_{p=L,R} \sum_k \epsilon_{pk} c_{pk}^\dagger c_{pk} + \sum_i E_i d_i^\dagger d_i; \quad (1)$$

$$H_1 = \sum_{pk} \sum_i V_{pi} c_{pk}^\dagger d_i + H.c.; \quad (2)$$

$H_0$  is the Hamiltonian for the isolated system of two leads and a quantum dot, and  $H_1$  is the tunneling Hamiltonian between a dot and two leads.  $E_i = \epsilon_i + E_g$  is the energy level of a dot which is shifted by the gate voltage ( $E_g$  is proportional to the gate voltage). The two metallic leads are conveniently named the left and right leads. The transmission amplitude for an electron moving from the left to right lead through the mesoscopic system can be expressed in terms of the mixed Green's function,

$$t_{RL}(\omega) = \frac{G_{RL}^r(\omega)}{2\rho_L \rho_R}; \quad (3)$$

where  $\rho_{L,R}$  is the density of states in the left (right) lead at the Fermi level. The mixed Green's function  $G_{RL}$  is

defined by

$$i\omega G_{RL}(t; t^0) = \sum_{kk^0} \text{Tr} c_{Rk}(t) c_{Lk^0}^\dagger(t^0); \quad (4)$$

The transmission amplitude through a quantum dot can be expressed in terms of the Green's function of the dot.

$$\frac{t_{AB}(\omega)}{2\rho_L \rho_R} = \sum_{ij} V_{Ri} D_{ij}^r(\omega) V_{jL}; \quad (5)$$

This transmission amplitude leads to the familiar expression of the transmission probability  $T(\omega) = |t_{AB}|^2$ .

$$T(\omega) = 4 \text{Tr} [D^r(\omega) D^a(\omega) g]; \quad (6)$$

$D^{r/a}$  is the retarded (advanced) Green's function of the dot. The Green's function of a noninteracting dot is given by the expression,

$$D^{r/a}(\omega) = [I - E - i\eta]^{-1}; \quad (7)$$

where  $E_{ij} = E_{iij}$  and  $i\eta = N_L V_{iL} V_{Lj} + N_R V_{iR} V_{Rj}$ . For this noninteracting dot, the transmission zeros of  $t_{AB}$  are sensitive to the relative phases of  $V_{Li}$  and  $V_{Ri}$ , since  $t_{AB}$  is the algebraic sum of  $D_{ij}$  weighted by the tunneling matrix elements.

An Aharonov-Bohm interferometer is made by introducing direct tunneling between the two leads,

$$H_2 = \sum_{kk^0} T_{LR} c_{Lk}^\dagger c_{Rk^0} + H.c.; \quad (8)$$

The transmission amplitude through the AB interferometer with an embedded quantum dot is given by the equation

$$\frac{t_{AB}(\omega)}{2\rho_L \rho_R} = \frac{T_{RL}}{1 + \eta} + \sum_{ij} V_{Ri} D_{ij}^r(\omega) V_{jL}; \quad (9)$$

Here  $\eta = 2N_L N_R |T_{LR}|^2$  is the dimensionless measure of the direct tunneling rate between the two leads and is related to the direct tunneling probability by  $T_0 = 4/(1 + \eta)^2$ . The tunneling matrix elements with a tilde can be considered as being renormalized by the direct tunneling:  $\tilde{V}_{iL} = [V_{iL} - i V_{Ri} N_R T_{RL}]/(1 + \eta)$  and  $\tilde{V}_{Ri} = [V_{Ri} - i T_{RL} N_L V_{Li}]/(1 + \eta)$ . The Green's function of the dot is also modified by the direct tunneling and the dot's self-energy is given by the expression:

$$\tilde{D}_{d;ij}^r = \sum_{p=L,R} \frac{N_p V_{ip} V_{pj}}{1 + \eta} + \frac{2N_L N_R}{1 + \eta} \sum_{p=L,R} V_{ip} T_{pp} V_{pj}; \quad (10)$$

Here the notation  $L = R$  and  $R = L$  is used. The effect of the Aharonov-Bohm flux threading through the AB interferometer can be taken into consideration by introducing the AB phase  $\phi = 2\pi\phi_0$  into the tunneling

matrix elements as  $V_{Ri}V_{iL}T_{LR} = \tilde{V}_{Ri}V_{iL}T_{LR}e^{i\phi_i}$ , where  $\phi_i = \hbar c/e$  is the flux quantum.

The behavior of the transmission phase depends sensitively on the relative phases of the tunneling matrix elements. In the time-reversal symmetric case, an electron's wave functions can be chosen to be real. For a real barrier potential, the tunneling matrix elements  $V_{pi}$  ( $p = L, R$ ) are thus all real. The signs of tunneling matrix elements can be introduced by the relations:

$$V_{Li} = s_{Li}\tilde{V}_{Li}; \quad V_{Ri} = s_{Ri}\tilde{V}_{Ri}; \quad (11)$$

Transforming the electron operator in the dot via

$$d_i \rightarrow s_{Li}d_i; \quad (12)$$

all the phases are ascribed to the right tunneling matrices. The left tunneling matrices are all positive,  $V_{Li} > 0$  for all  $i$ 's, and

$$V_{Ri} = s_i\tilde{V}_{Ri}; \quad s_i = s_{Li}s_{Ri}; \quad (13)$$

where  $s_i = \pm 1$ . We have no information about the distribution of  $s_i$  at this point. Though the tunneling matrix elements are all assumed to be real, the conclusion remains the same as long as the relative phases between the left and right tunneling matrix elements are real. An overall random phase in the left and right tunneling matrices does not change the physics.

### III. TRANSMISSION PHASE AND DISTRIBUTION OF RELATIVE SIGNS IN TUNNELING MATRIX ELEMENTS

In this section, we consider several possible distributions of the relative signs in the left and right tunneling matrix elements and study the behavior of the transmission zeros and phase. We end the general rule which governs the relationship between the signs and the transmission phase. The transmission probability through a dot takes on many different shapes depending on the distribution of the signs. A closed or unitary AB interferometer with an embedded quantum dot can thus be an auxiliary experimental probe to measure the transmission zeros and phase.

Before presenting our results, we briefly comment on the validity of our single-particle approach to a quantum dot. The transmission probability through a quantum dot in a two-terminal configuration is the sum of the Green's functions of the dot weighted by the tunneling matrix elements [see Eq. (5)]. The poles in the Green's functions are determined by the zeros of the determinant  $[\mathbb{D}^x]^{-1}$ . Though the position of the zeros in the determinant depends on the relative signs of the tunneling matrix elements, the existence of zeros in the determinant is not sensitive to the relative signs. On the other hand, the existence of the transmission zeros in  $t_0$  is sensitively determined by the relative signs of the tunneling

matrix elements. At the level of the Hartree approximation, the main effect of the Coulomb interaction is to make discrete poles which are separated by the Coulomb interaction plus the difference in the single-particle energy spectrum. The level broadening is mainly determined by the tunneling into two leads. Since Eq. (5) is valid at the level of the Hartree approximation, we believe the transmission zeros are still determined by the relative signs of the tunneling matrix elements, although we do not consider this case explicitly here.

We would like to emphasize that our consideration of the distributions of the relative signs in the left and right tunneling matrix elements do have physical realizations. To obtain the information about the tunneling matrix elements requires the solution of the Schrodinger equation for the entire structure of a quantum dot and two leads. Simplifying the system to the one-dimensional problem, there have been some approaches to computing the transmission amplitude of the quantum dot system. Modeling the quantum dot by a double-barrier well (DBW) or t stub, plane waves are matched at the boundaries between the quantum dot and the two leads. The structure of the transmission amplitude for the DBW (t stub) is completely equivalent to the case of the oscillating (uniform) distribution of the relative signs, as will be discussed below. The stepwise distribution of the relative signs is also possible for the double-barrier t stub system.

For our model study, we assume the quantum dot is described by a uniform single-particle energy spectrum with energy spacing  $\epsilon$ . The level spacing implicitly includes the effect of the Coulomb interaction at the Hartree approximation level. We keep a finite number of energy levels with  $i = 1$  where the integer  $i$  is constrained to  $N - i \leq N$  and  $N = 50$  is chosen in our plots. The transmission probabilities  $T_0(0)$  of a quantum dot,  $T_{AB}(0)$  of an AB interferometer at the Fermi energy  $\epsilon_F = 0$ , and the transmission phase  $\phi$  of a quantum dot are computed as a function of the energy shift  $E_g$  by the gate voltage. In most of the presented figures,  $E_g$  is varied from  $-\epsilon/4$  to  $\epsilon/4$ . This energy range covers 9 discrete energy levels of the dot. Unless otherwise noted, we use the same set of the tunneling matrix elements to emphasize the effects of  $s_i$ 's. The values of  $s_{Li} = (s_{Ri})$  for  $i = 1, \dots, N$ ;  $N + 1, \dots, 2N$  are chosen randomly between 0.01 (0.03) and 0.02 (0.06), respectively, where  $t_{pi} = N_p V_{pL} V_{Li}$  for  $p = L, R$ . When the quantum dot is embedded into one arm of an AB interferometer, the effect of the AB flux is taken into account by introducing an AB phase  $\phi_{AB}$  into the tunneling matrices. Though the energy spectrum and the tunneling matrix elements of a dot are modified by magnetic fields (see Sec. IV), our presented figures are computed using a rigid energy spectrum and rigid tunneling matrix elements.

To begin we consider the case when all the relative signs are equal, i.e.,  $s_i = 1$  for all  $i$ 's. The transmission probability  $T_0$  of the quantum dot is displayed for this case in Fig. 1 (a).  $T_0$  has a repeating sequence of zero-pole pairs. The transmission probability is peaked

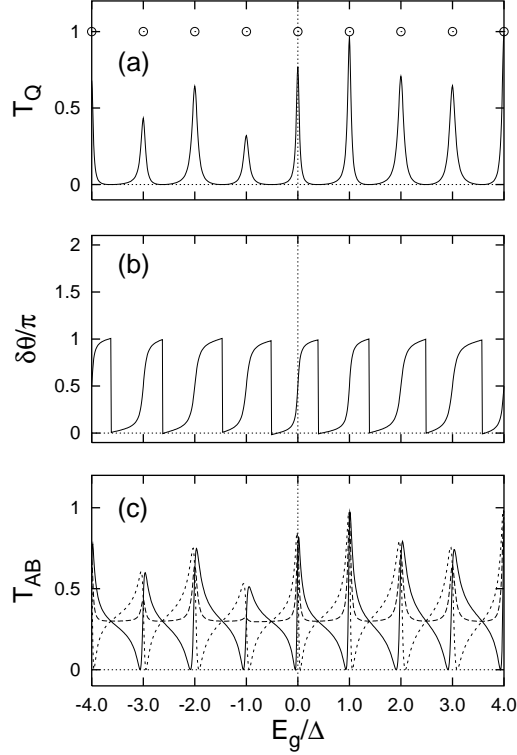


FIG. 1: Uniform distribution of relative signs ( $s_i = 1$ ). (a) The transmission probability  $T_Q$  of a quantum dot. Open circles denote the relative signs of the tunneling matrix elements.  $s_i = 1$  when an open circle is located at 1 (0) on the y-direction, respectively. (b) The variation of the transmission phase. (c) When the quantum dot is embedded into the Aharonov-Bohm interferometer, the Fano interference pattern shows up in the transmission probability  $T_{AB}$ . The AB phase ( $\phi$ ) dependence of  $T_{AB}$  is displayed ( $T_0 = 0.3$ ): solid line ( $\phi = 0$ ), long dashed line ( $\phi = 90$ ), and short dashed line ( $\phi = 180$ ).

whenever the Fermi energy is aligned with one of discrete energy levels in the dot.  $T_Q$  is zero at the transmission zeros, which lie in between two neighboring transmission peaks or poles. The change in the transmission phase,  $\delta\theta$ , is displayed in Fig. 1 (b).  $\delta\theta$  increases by  $\pi$  over every transmission peak and jumps by  $\pi$  at transmission zeros.  $\delta\theta$  shows an oscillating behavior: an increase over poles and a drop at zeros. The transport properties of this quantum dot system are very similar to those of well-studied stub system.<sup>6,7,10</sup>

When the quantum dot is embedded in an AB interferometer, the transmission probability  $T_{AB}$  shows Fano interference<sup>11</sup> between the direct tunneling and the resonant path through the dot. As shown in Fig. 1 (c), a repeating sequence of zero-pole pairs (solid line) still remains and additional zeros are not generated by the destructive Fano interference. The asymmetric Fano resonance shape in  $T_{AB}$  for each peak are equivalent or "in phase" in the sense that they are modulated in the same

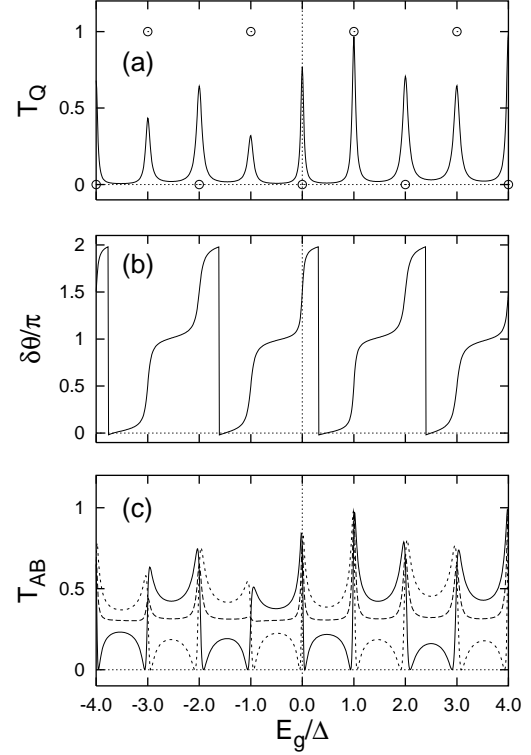


FIG. 2: Oscillating distribution of relative signs ( $s_i = (-1)^{i+1}$ ). The integer  $i$  labels the single-particle energy levels in a dot. (a)  $T_Q$  at the Fermi energy. The meaning of open circles are explained in the caption of Fig. 1. (b) The transmission phase. For display,  $\delta\theta$  is folded into the range  $[0; 2\pi]$  so that the apparent jump of  $\delta\theta$  by  $2\pi$  should be understood as continuous line. (c)  $T_{AB}$  in an AB ring. Lines are the same as in Fig. 1.

way by the AB flux.  $T_{AB}(\phi = 0)$  has an N-shape structure, and the shape of  $T_{AB}$  is transformed into an inverse N-shape when  $\phi = 180$ . The transmission zeros of  $T_{AB}$  lie on the real-energy axis when  $\phi = n\pi$ , where  $n$  is an integer. For other values of the AB phase  $\phi$ , the transmission zeros become complex. Due to the Onsager relation,  $T_{AB}(\phi)$  is equal to  $T_{AB}(\phi + \pi)$ .

In recent measurements of the transmission phase,  $\delta\theta$ , of a quantum dot in an open AB interferometer, oscillating behavior of  $\delta\theta$  was observed over several Coulomb peaks. Within our model, these experimental features can be explained when the relative signs of the tunneling matrix elements are all equal.

When the relative signs of the tunneling matrix elements are oscillating from level to level,  $s_i = (-1)^{i+1}$ , the structure of transmission zeros is drastically modified. There are no transmission zeros in  $T_Q$ , but instead  $T_Q$  has a series of transmission poles. Since no transmission zeros exist in  $T_Q$ , the transmission phase steadily increases by  $\pi$  as the energy levels of the dot are scanned by varying  $E_g$  through the Fermi level of the leads. The behavior of this quantum dot system is very similar to a

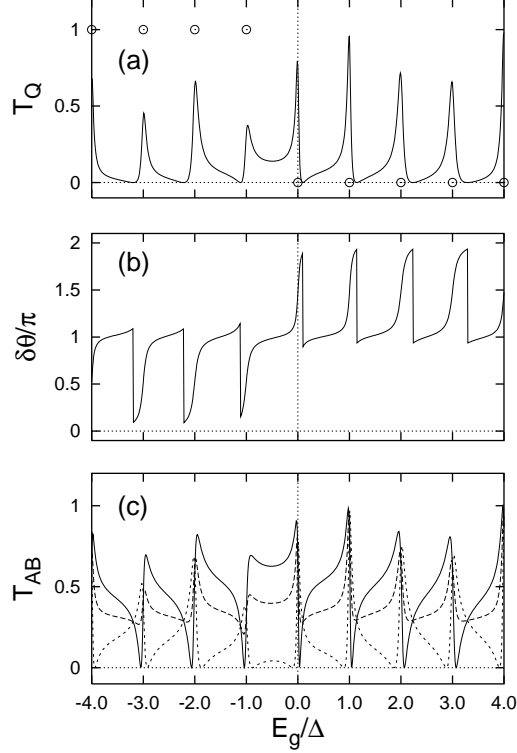


FIG. 3: Stepwise distribution of relative signs ( $s_i = 1$  for  $i = 1$  and  $s_i = -1$  for  $i = 0$ ). (a) The asymmetrical lineshape in  $T_Q$  arises from the combined effects of the stepwise distribution of relative signs and the interference between multiple energy levels. (b) One transmission zero is removed in the boundary energy range  $-1 < E_g = 0$ . (c)  $T_{AB}$  in an AB ring. Lines are the same as in Fig. 1.

double-barrier well and double-barrier resonant tunneling system<sup>6,7,10</sup>

When this quantum dot is inserted into an AB interferometer, destructive Fano interference generates transmission zeros in  $T_{AB}$  in an energy interval of  $E_g$  where  $T_Q$  has no zeros.  $T_{AB}$  has a repeating sequence of zero-zero-pole-pole structure. Although the difference in the  $T_Q$ 's is not significant between the two distributions of  $s_i$ 's in Fig. 1(a) and Fig. 2(a), the shapes of  $T_{AB}$  are quite different. In this case  $T_{AB}$  consists of a repeating sequence of the structure of M-shape and W-shape when  $\phi = 0$ . The M (W)-shape is transformed into the W (M)-shape when  $\phi = 180^\circ$ . The difference in Fig. 1(c) and Fig. 2(c) suggests that these two types of distributions in  $s_i$ 's can be distinguished by measuring the linear response conductance  $G_{AB}$  in the AB interferometer with an embedded quantum dot and by inspecting the shapes of  $G_{AB}$  as a function of the gate voltage and magnetic field.

We further explore other possible distribution of  $s_i$ 's. The behavior of  $T_{Q,AB}$  and  $\delta\theta$  are displayed in Fig. 3 when  $s_i = 1$  for  $i = 1$  and  $s_i = -1$  for  $i = 0$ . In this stepwise distribution of the relative signs, the transmission phase

show the expected oscillating behavior due to transmission zeros [see Fig. 1(b)] in the two energy ranges of uniform relative signs [see Fig. 3(b)]. However, one transmission zero is removed in the energy interval which lies in between the two energy levels whose signs ( $s_i$ ) are opposite. Removal of one zero leads to a continuous increase of  $\delta\theta$  over each energy level ( $E_g = 0$  and  $E_g = 0$  in our model calculation). As displayed in Fig. 3(a), the shape of  $T_Q$  is now asymmetrical with respect to each peak position. Furthermore, the shape of  $T_Q$  in both energy regions of uniform signs is different by a "phase" in the sense that the AB phase can change the shape of  $T_{AB}$  in one region into that of  $T_{AB}$  in the other, and vice versa [See Fig. 3(c)]. Obviously this phase change in  $T_Q$  stems from the sign flip in the tunneling matrix elements. The absence of one transmission zero in  $T_Q$  is much more apparent in  $T_{AB}$ .

We now consider the cases that all the energy levels have the same relative signs except for one energy interval with the flipped relative signs. The energy levels belonging to this flipped energy interval have the opposite relative signs,  $s = -1$ , compared to all the other levels with  $s = 1$ . In Fig. 4 (a) and (b), we study  $T_{Q,AB}$  and  $\delta\theta$  when the flipped energy interval consists of only one level,  $i = 0$ . Transmission zeros are removed only in the energy range lying in between the two levels with the opposite signs. Since no zeros exist for  $E_g = 0$ , the transmission phase increases by  $\pi$  over each level  $i = 1; 0; 1$ . The shape of  $T_Q$  is similar to the case of uniform distribution of  $s_i$ 's except for the removal of transmission zeros. On the other hand  $T_{AB}$  ( $\phi = 0$ ) is significantly modified in the flipped energy interval. As the number of the flipped levels is increased, transmission zeros are removed only in the energy range lying in between the two levels with opposite signs or in the interface energy range between the flipped interval and the rest. Transmission zeros and the corresponding phase jumps persist in between two levels with the same relative signs. The case when the flipped interval consists of three levels is studied in Fig. 4 (c) and (d). Examination of  $T_{AB}$  reveals that the "phase" of  $T_{AB}$  is different between the inside and outside of the flipped interval. The interval acts to shift the phase by  $\pi$  at the two boundaries, and the shape of  $T_{AB}$  is identical on both sides of the flipped interval.

When the line-broadening is much smaller than the interlevel spacing, we can deduce from these results the following rules for the behavior of the transmission zeros. When the relative signs are opposite for the two neighboring energy levels, the transmission zero is absent in the energy interval bounded by two levels. When the relative signs are the same for two neighboring energy levels, one transmission zero is generated inside the energy interval bounded by two levels. This conclusion can be modified when one of the linewidth matrix elements is by far larger than the others as will be shown below.

The lineshape in  $T_Q(E_g)$  can be asymmetrical depending on the relative signs of the tunneling matrix elements

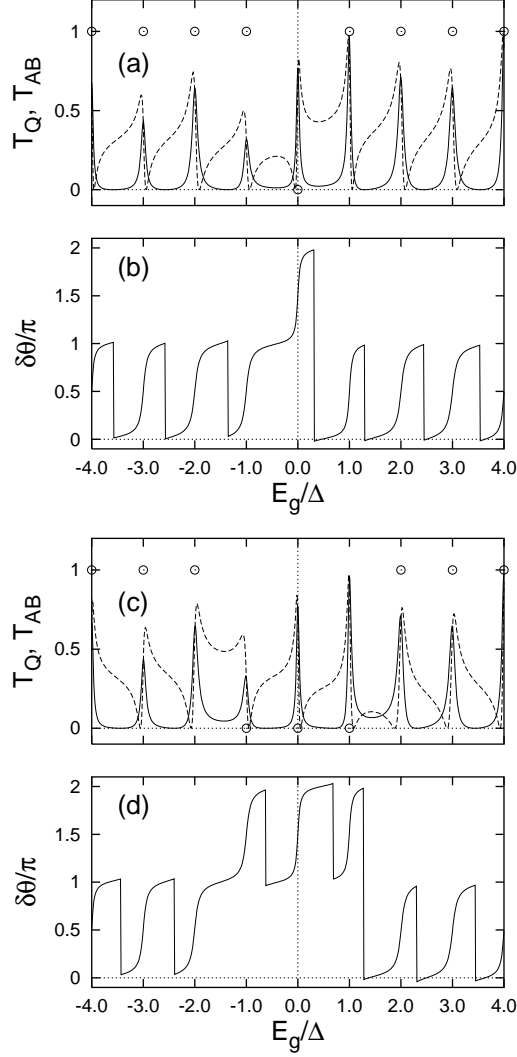


FIG. 4: Uniform relative signs ( $s_i = 1$ ) except for one flipped sign ( $s_i = -1$ ). (a) and (c): Transmission probabilities  $T_Q$  (solid line) and  $T_{AB}$  (dashed line). (b) and (d): The transmission phase of a dot. The jump by 2 should be understood as a continuous line because the phase is defined to be between 0 and  $2\pi$ .

and their magnitude. One example of an asymmetrical lineshape is already displayed in Fig. 3 for the stepwise distribution of relative signs. Another way to make the lineshape of  $T_Q$  asymmetrical is to make one energy level more strongly coupled to the two leads than the other levels. This strongly coupled level is broadened and can act as an effective continuum band to other narrow levels. The interference between the broad level and the narrow levels leads to the asymmetrical Fano lineshape. A typical example is displayed in Fig. 5 when the relative signs in the tunneling matrix elements are equal for all energy levels. Although the lineshape in  $T_Q$  is modified compared to Fig. 1, the transmission zeros for the uniform distribution of signs persist.

In addition to the asymmetrical lineshape, a more dra-

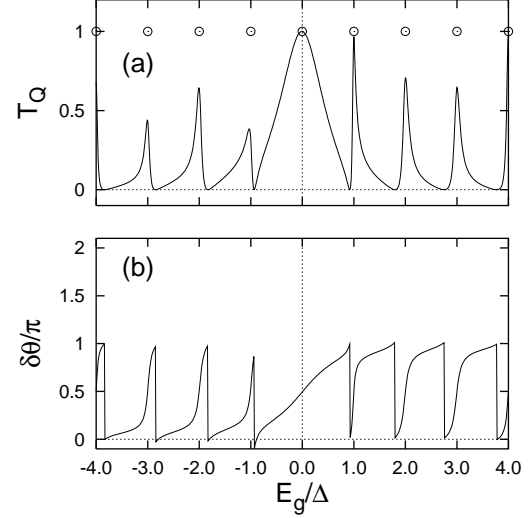


FIG. 5: (a) Transmission probability  $T_Q$  and (b) transmission phase for a dot when the relative signs are uniform and one energy level is much more strongly coupled to two leads than the other energy levels. Even with the same relative signs for all energy levels, the lineshape is asymmetrical. Model parameters are the same as in the previous figures except that one of the line broadening parameters,  $\Gamma_{L,R}$  for  $i = 0$ , is chosen to be large:  $\Gamma_{L0} = \Gamma_{R0} = 2$ .

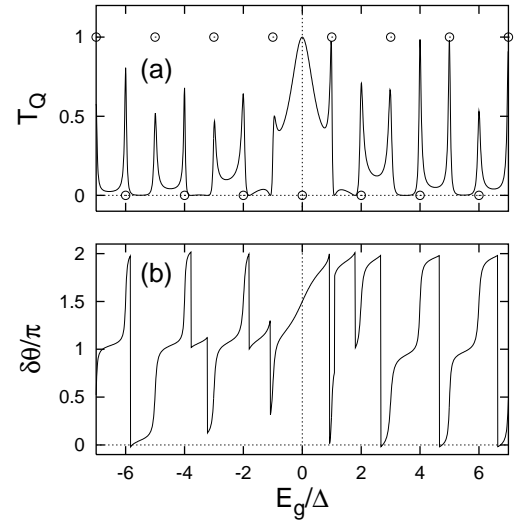


FIG. 6: (a) Transmission probability  $T_Q$  and (b) transmission phase for a dot when the relative signs are oscillating from level to level and one energy level is much more strongly coupled to two leads than the other energy levels. Model parameters are the same as in Fig. 5. Note the far-reaching effect of the strong coupling for one level on the other levels. The jump by 2 in should be understood as a continuous line.

matic effect of Fano interference (see Fig. 6) can occur in the transmission zeros when the relative signs are oscillating from one level to the next. As shown in Fig. 2, the transmission zeros are absent for the oscillating distribution of signs when the linewidth is much smaller than the interlevel spacing. Surprisingly, new transmission zeros are generated due to Fano interference between the broad energy level and the other narrow levels. Note that the strong coupling of one level to the leads is very far-reaching and has the same effect on the structure of the transmission amplitude as the AB interferometer.

#### IV. MODEL CALCULATION OF RELATIVE SIGNS

In the previous section, we studied the transmission zeros and phase of a quantum dot for several possible distributions of the relative signs in the tunneling matrix elements. A uniform distribution of signs is consistent with recent experimental results. In this section we present a simple scenario which can lead to a uniform distribution of signs.

The single-particle energy-level spectrum in a quantum dot has been inferred by monitoring the position of the Coulomb-regulated conductance peaks as a function of magnetic field<sup>12</sup>. After subtracting the Coulomb interaction from the difference between two conductance peaks, the single-particle energy spectrum was inferred and well-described by the Fock-Darwin energy levels for some range of magnetic fields. In this section we show that the Fock-Darwin energy spectrum<sup>13,14</sup> of a quantum dot can lead with some modest assumptions to a uniform distribution of the signs of the tunneling matrix elements.

Consider a quantum dot which is defined in a 2D electron system by the circular harmonic confinement potential

$$V_c(\mathbf{x};y) = \frac{1}{2} m_e \omega_0^2 (x^2 + y^2); \quad (14)$$

Here  $m_e$  is the electron's mass and  $\omega_0$  is the energy scale of the confining potential. The quantum dot is taken to be weakly coupled by tunneling to two leads which can be described by one transport channel. The tunneling between the two systems is assumed to be weak enough not to modify the electron's wave functions except for broadening the lineshapes. The Coulomb interaction in a dot is treated semiclassically. With these assumptions the single-particle energy spectrum in the presence of perpendicular magnetic fields is given by the Fock-Darwin spectrum,

$$E(n;m) = (2n + |m| + 1) \hbar \omega_0; \quad (15)$$

and the wave functions are

$$\psi_{nm}(\mathbf{x};y) = N_{nm} e^{im\phi} e^{-\frac{1}{2} \frac{m}{\ell_B} y} L_n^{|m|} \left( \frac{y^2}{\ell_B^2} \right); \quad (16)$$

Here  $N_{nm} = \frac{1}{\sqrt{a^2 (n+|m|)!}} \frac{n!}{n!}$  is a normalization constant,  $n$  is the nonnegative integer, and  $m$  is an integer. The other variables in this equation are  $\ell_B = a$  with  $a = \sqrt{\hbar / m_e \omega_0}$ ,  $\omega_0 = \sqrt{2} \omega_c$ , and  $\omega_c = eB / m_e c$ . In the absence of magnetic fields, the energy spectrum reduces to

$$E_N = (N + 1) \hbar \omega_c; \quad N = 2n + |m|; \quad (17)$$

Each energy level  $E_N$  is degenerate with  $D_N = N + 1$ , where  $N = 0; 1; 2; \dots$ .

We now discuss the structure of the tunneling matrix elements. The tunneling barrier is assumed to be described by a real potential, even in a magnetic field. To study simply oscillating phase-coherent transport, the two leads should accommodate only one transport channel. Leads with more than one channel will show more complex patterns in the AB oscillations. For a circularly symmetric quantum dot, the radial part of the wave function determines the overall magnitude of the tunneling matrix elements but plays no role in determining their phase. The phase of the tunneling matrix elements is determined solely by the angular part of the wave function. For an ideal point contact between the two leads and the quantum dot with one lead at  $\phi = 0$  and the other lead at  $\phi = \pi$ , the relative phase between the left and right tunneling matrix elements for the energy level labeled by  $(n;m)$  is given by  $e^{im\pi} = (-1)^m$ . The ideal point contact condition can be relaxed. If  $\phi = 0$  is replaced by  $\phi = \pi/2$  and  $\phi = \pi$  is replaced by  $\phi = 3\pi/2$ , then for the constant tunneling over this range of  $\phi$ , the relative phase is  $(-1)^m$  times the signs of  $\sin m\pi/2 = \sin m\pi/2$ . As long as  $\pi/2 = \pi/2$ , the relative phase is  $(-1)^m$  for reasonable values of  $m$ .

In the absence of a magnetic field, any energy level consists of degenerate states with only even  $m$  or only odd  $m$ . The angular part of wavefunctions can be made real by the appropriate linear combinations of degenerate wavefunctions. The relative signs are still given by  $(-1)^m$ . The energy levels of even  $m$  and odd  $m$  alternate with increasing energy. In a semiclassical approach to the Coulomb interaction, an electron added to the quantum dot will occupy the single-particle states which are unoccupied and lowest in energy. Until one single particle energy level  $E_N$  is exhausted by  $2(N + 1)$  electrons (including the spin degeneracy), the relative phases or signs will be equal so that the transmission zeros are generated in between the transmission peaks. When the next higher energy level  $E_{N+1}$  starts to be filled, the relative phase is now opposite to that of the lower energy level  $E_N$ . When  $E_g$  is varied from the last electron filling at  $E_N$  to the first electron filling at  $E_{N+1}$ , there will not be a transmission zero. Successive transmission zeros start to appear again in the transmission amplitude while the energy level  $E_{N+1}$  is filled by electrons. The absence of the transmission zeros is realized only when going from  $E_N$  to  $E_{N+1}$ .

In the presence of a magnetic field, time-reversal symmetry is broken and the wavefunctions cannot be chosen

to be real. The relative signs are still  $(-1)^n$  for the state  $(n; m)$  if the tunneling barrier potential is real and the electron's wavefunction in the one-channel leads are not modified in the presence of magnetic fields. The transmission phase will behave in the same way as for  $B = 0$  when the magnetic field is weak enough for level-crossing not to occur. In a strong magnetic field, energy level-crossing starts to occur and the distribution of the relative signs is modified as well. We believe that keeping track of the relative signs is possible experimentally just like monitoring the Coulomb peaks in the conductance. When the magnetic field is strong enough that only the lowest Landau level is filled, the energy levels will be ordered with an increasing azimuthal quantum number  $m$ . For this case, the relative signs will oscillate from level to level. However, the spin-degeneracy can double the oscillating period in the relative signs.

## V. CONCLUSION

In this paper we considered several possible distributions of the relative signs in the tunneling matrix elements and studied the effects of these signs on the transmission zeros and phase. When the tunneling matrix elements are much smaller than the interlevel spacing or the distance between the Coulomb peaks, we find the following general rules governing the relation between the relative signs and the transmission zeros or phase. When the relative signs are opposite for the two neighboring energy levels, a transmission zero is absent in the energy interval bounded by the two levels. When the relative signs are the same for two neighboring energy levels, one transmission zero is generated inside the energy interval bounded by two levels. Silva, et. al.<sup>8</sup> studied a quantum dot with two energy levels and found these same results. In our work we find that the above two rules are generally true even in the presence of other energy levels in a dot, as far as the linewidths are much smaller than the energy level spacing. Based on the above two rules, we can predict the behavior of the transmission zeros and phase from the distribution of the relative signs. A uniform distribution of signs within some energy interval leads to transmission zeros in between any pair of conductance peaks. The oscillating distribution of signs completely removes the transmission zeros.

When the strength of the tunneling matrix elements becomes larger comparable to the interlevel spacing, the above simple rules are modified. One example is when one energy level is coupled much more strongly to the two leads than other levels. When the strongly coupled level is broad enough to cover several neighboring energy levels, this broad level can act as the continuum band to the neighboring narrow levels and Fano interference occurs. The Fano interference results in an asymmetrical lineshape as well as the generation of new transmission zeros which are otherwise absent.

Since we did not take into account in full length the

Coulomb interaction between electrons in the quantum dot, some care is needed to apply our theoretical results to the real quantum dots. In the Hartree approximation, the Coulomb energy mainly shifts the chemical potential or determines the poles of the Green's function of a dot. When the tunneling matrix elements are so small that the Coulomb blockade peaks are well separated and narrow, our theory will be relevant to the experiments.

We have emphasized that the transmission zeros can be located by inspecting the Fano interference shape in  $T_{AB}$  as a function of the gate voltage and the magnetic field. The AB phase shifts the transmission zeros off the real-energy axis and modulates the shape of  $T_{AB}$ . Depending on the existence or the absence of the transmission zeros in  $T_Q$ , the variation of  $T_{AB}$  with the gate voltage is quite different. There is one experiment<sup>15</sup> in which the linear conductance or  $T_{AB}$  of the AB interferometer with an embedded quantum dot was measured. Based on our results [see Fig. 3 (c)], we can conclude that the signs of the tunneling matrix elements are flipped in the gate voltage range  $0.05\text{V} < V_g < 0\text{V}$  of Fig. 1 (a) in the work<sup>15</sup> of Kobayashi, et. al. Furthermore, all the energy levels covered by the gate voltage  $0.15\text{V} < V_g < 0.05\text{V}$  seem to have the same relative signs in the tunneling matrix elements. The measured variation<sup>15</sup> of the conductance  $G_{AB}$  in Fig. 4 (a) is well reproduced by our  $T_{AB}$ 's for a uniform distribution of the relative signs.

Our study shows that the asymmetrical lineshape of  $T_Q(E_g)$  can result from the interference between the transport channels through the energy levels in a dot. Some experimental groups<sup>16,17</sup> have observed an asymmetrical lineshape of  $G_Q(E_g)$  as a function of the gate voltage. This feature may be understood in terms of the interference between multiple energy levels in a dot and the distribution of the relative signs in the tunneling matrix elements.

In summary, we studied the relationship between the transmission phase and the signs of the tunneling matrix elements. The behavior of the transmission zeros and phase is very sensitively dependent on distribution of the relative signs between the left and right tunneling matrix elements, and on their strength. We suggest that the location of the transmission zeros can be identified by inspecting the shape of the conductance as a function of the gate voltage in the closed AB interferometers.

## Acknowledgments

This work was supported in part by the National Science Foundation under Grant No. DMR 9357474, in part by the BK 21 project, and in part by grant No. 1999-2-114-005-5 from the KOSEF.



# APPENDIX A: COMPLEX FANO FACTOR IN THE AHARONOV-BOHM RING WITH AN EMBEDDED QUANTUM DOT

Asymmetric Fano lineshapes in the conductance have been observed in transport through the mesoscopic systems.<sup>15,16,17</sup> The AB interferometer with an embedded quantum dot<sup>15</sup> is one such system. In the main text we have already studied Fano interference patterns in the conductance of an AB ring. In this appendix we are going to show that the complex Fano factor is closely related to the complex transmission zeros in  $t_{AB}$  or the transmission amplitude of an AB ring. The complex Fano factor is an oscillatory function of the magnetic fields threading through an AB ring.

As Fano proposed<sup>11</sup>, asymmetric Fano lineshapes arise from the interference between the continuum energy spectrum and one discrete energy level.

$$F(x) = F_1 \frac{(x + q)^2}{x^2 + 1}; \quad (A1)$$

Here  $q$  is the asymmetric Fano factor and is real in most cases. The Fano resonance is featured with a pair of one dip and one peak structures, which is in direct contrast with the Lorentzian shape of a one peak structure.

To simplify the algebra and to make the physics clear, we consider a model quantum dot which is described by one resonant level. In this case Eq. (9) is simplified as

$$t_{AB} = \frac{(\epsilon_d) \frac{P}{T_0} + \frac{-P}{g} \cos \phi + i \frac{-P}{g} \sin \phi}{\epsilon_d + \frac{-P}{g} \cos \phi + i}; \quad (A2)$$

The overall phase is removed from  $t_{AB}$  and  $\epsilon_d$  is the resonant energy level. The direct tunneling probability  $T_0$  is given by the expression  $T_0 = 4/(1 + \beta)^2$ , where  $\beta = 2N_L N_R \mathcal{J}_{LR}^2$ ,  $\beta = (\beta_L + \beta_R) = (1 + \beta)$ , and  $g = 4\beta_L \beta_R = (\beta_L + \beta_R)^2$  with  $\beta_{L=R} = N_{L=R} \mathcal{J}_{L=R}^2$ .

Writing  $Z = \epsilon_d$ , we can rewrite  $t_{AB}$  in terms of the pole  $Z_p$  and the zero  $Z_z$  as

$$t_{AB} = \frac{P}{T_0} \frac{Z_z}{Z} \frac{Z_p}{Z_p}; \quad (A3)$$

This zero-pole pair is given by the expressions,

$$Z_p = \frac{-P}{r} \frac{g}{\cos \phi} - i; \quad (A4a)$$

$$Z_z = -\frac{g}{T_0} [\cos \phi + i \sin \phi]; \quad (A4b)$$

Writing  $x = (\epsilon_d) = \frac{\epsilon_d}{T_0}$ , the transmission probability  $T_{AB} = |t_{AB}|^2$  becomes

$$T_{AB} = T_0 \frac{(\beta + q(\phi))^2}{(\beta + \frac{P}{g} \cos \phi)^2 + 1}; \quad (A5)$$

where  $q(\phi) = Z_z(\phi) = \frac{q}{T_0} e^{i\phi}$  is the complex asymmetric Fano factor.  $T_{AB}$  is of the same form as Eq. (A1) except that the asymmetric Fano factor is now a complex number depending on the AB phase  $\phi$ . The asymmetric Fano factor is proportional to the transmission zero of the AB ring. The absolute magnitude of  $q$ ,  $|q| = \frac{g}{T_0}$ , is independent of the magnetic field in the case of one resonant level model.

When the quantum dot is modeled by multiple resonant levels, the basic features of one resonant level model are not modified. The complex transmission zeros in  $t_{AB}$  become purely real when  $\phi = n\pi$  with an integer  $n$ . Though the imaginary part of the zeros in  $t_{AB}$  is still sinusoidal as a function of  $\phi$ , its functional form is not given by the form  $\sin \phi$ .<sup>7</sup> The absolute value of the complex Fano factor in this case is weakly dependent on magnetic field.

- <sup>1</sup> A. Yacoby, M. Heiblum, D. Mahalu, and H. Shtrikman, Phys. Rev. Lett. 74, 4047 (1995).
- <sup>2</sup> R. Schuster, E. Buks, M. Heiblum, D. Mahalu, V. Umansky, and H. Shtrikman, Nature 385, 417 (1997).
- <sup>3</sup> Y. Ji, M. Heiblum, D. Sprinzak, D. Mahalu, and H. Shtrikman, Science 290, 779 (2000).
- <sup>4</sup> Y. Ji, M. Heiblum, and H. Shtrikman, Phys. Rev. Lett. 88, 076601 (2002).
- <sup>5</sup> H.-W. Lee, Phys. Rev. Lett. 82, 2358 (1999).
- <sup>6</sup> T. Taniguchi and M. Buttiker, Phys. Rev. B 60, 13814 (1999).
- <sup>7</sup> T.-S. Kim, S.-Y. Cho, C.-K. Kim, and C.-M. Ryu, Phys. Rev. B 65, 245307 (2002).
- <sup>8</sup> A. Silva, Y. Oreg, and Y. Gefen, Phys. Rev. B 66, 195316 (2002).
- <sup>9</sup> Y. Gefen, cond-mat/0207440.
- <sup>10</sup> Z. Shao, W. Porod, and C. S. Lent, Phys. Rev. B 49, 7453

- (1994).
- <sup>11</sup> U. Fano, Phys. Rev. 124, 1866 (1961).
- <sup>12</sup> P. L. McEuen, E. B. Foxman, U. Meirav, M. A. Kastner, Y. Meir, N. S. Wingreen, and S. J. Wind, Phys. Rev. Lett. 66, 1926 (1991).
- <sup>13</sup> V. Fock, Z. Phys. 47, 446 (1928).
- <sup>14</sup> C. G. Darwin, Proc. Cambridge Philos. Soc. 27, 86 (1930).
- <sup>15</sup> K. Kobayashi, H. Akawa, S. Katsumoto, and Y. Iye, Phys. Rev. Lett. 88, 256806 (2002).
- <sup>16</sup> J. Gores, D. Goldhaber-Gordon, S. Heemeyer, M. A. Kastner, H. Shtrikman, D. Mahalu, and U. Meirav, Phys. Rev. B 62, 2188 (2000).
- <sup>17</sup> I. G. Zacharia, D. Goldhaber-Gordon, G. G. Ranger, M. A. Kastner, Yu. B. Kharin, H. Shtrikman, D. Mahalu, and U. Meirav, Phys. Rev. B 64, 155311 (2000).